Static magnetic order in metallic triangular antiferromagnet Ag_2MnO_2 detected by muon-spin spectroscopy

Jun Sugiyama,[1,*] Hiroshi Nozaki,[1] Yutaka Ikedo,[1] Kazuhiko Mukai,[1] Peter L. Russo,[2] Daniel Andreica,[3] Alex Amato,[4] Hiroaki Yoshida,[5] and Zenji Hiroi[5]

[1]*Toyota Central Research and Development Laboratories Incorporated, Nagakute, Aichi 480-1192, Japan*

[2]*TRIUMF, 4004 Wesbrook Mall, Vancouver, BC, V6T 2A3 Canada*

[3]*Faculty of Physics, Babes-Bolyai University, 3400 Cluj-Napoca, Romania*

[4]*Laboratory for Muon Spin Spectroscopy, Paul Scherrer Institut, CH-5232 Villigen PSI, Switzerland*

[5]*ISSP, University of Tokyo, 5-1-5 Kashiwanoha, Kashiwa 277-8581, Japan*

(Received 16 April 2008; revised manuscript received 6 September 2008; published 30 September 2008)

The magnetic nature of the triangular antiferromagnet Ag_2MnO_2, which exhibits two magnetic transitions at $T_{m1}\sim 80$ K and $T_{m2}\sim 30$ K, has been studied with positive muon-spin rotation and relaxation (μ^+SR) spectroscopy using a polycrystalline sample in the temperature (T) range between 300 and 1.8 K. Weak transverse-field μ^+SR measurements suggest the appearance of a random internal magnetic field at T below T_{m1}, while zero-field (ZF) μ^+SR measurements indicate the existence of static internal magnetic fields below T_{m2}. Furthermore, two components with ~10 times different precession frequencies but almost equivalent amplitudes in the ZF spectrum indicate the formation of a static but complex antiferromagnetic order below T_{m2}. The overall magnetic behavior is therefore clarified that the disordered moments appear below $T_{m1}=T_N^{on}$, whereas static short-range antiferromagnetic order completes below $T_{m2}=T_N^{end}$.

DOI: 10.1103/PhysRevB.78.104427 PACS number(s): 76.75.+i

I. INTRODUCTION

Layered transition-metal dioxides AMO_2 [which consist of alternating stacks of A and MO_2 planes, where A^+ stands for an alkali (Li^+, Na^+, K^+, Rb^+, and Cs^+), Ag^+ or $(Ag_2)^+$ ion and M^{3+} for a transition-metal ion, and in which M ions form a two-dimensional triangular lattice (2DTL) by connection of edge-sharing MO_6 octahedra] have been heavily investigated due to their complex magnetic behavior[1–4] and a recent discovery of superconductivity in the hydrated sodium cobalt dioxides $Na_xCoO_2*1.3H_2O$.[5] Although the 2D interaction is thought to play an essential role in determining the magnetic nature of AMO_2, the interplane [three-dimensional (3D)] interaction sometimes contributes to form long-range order in the AMO_2 compounds. Here, we call the AMO_2 with relevant interactions as "quasi-2D" compounds.

For $NaNiO_2$ and $Na_{0.75}CoO_2$, the A-type antiferromagnetic (AF) order, i.e., ferromagnetic (FM) order in the NiO_2 (CoO_2) plane but AF order between the two adjacent NiO_2 (CoO_2) planes, was detected by neutron-diffraction experiments.[6–9] Nevertheless, the majority of past theoretical models are developed on the pure 2D system—i.e., the 2DTL separated from the adjacent 2DTLs by an infinite distance and ignored the 3D interactions.[10–14] This is because, since the 3D interaction naturally introduces an additional degree of freedom, it is very difficult to predict the magnetic nature of the quasi-2D compounds. On the other hand, in order to reduce the 3D interaction and to make the quasi-2D compounds close to an ideal 2D system, one could increase the interplane distance (d_{IP}) of AMO_2 by using A ions with larger ionic radius. In particular, the largest d_{IP} is achieved for $A=Ag_2$ for AMO_2, when M is Ni; that is, $d_{IP}=0.473$ nm for $LiNiO_2$,[15] 0.52 nm for $NaNiO_2$,[7] 0.612 nm for $AgNiO_2$,[16] and 0.801 nm for Ag_2NiO_2 (Ref. 17) but $KNiO_2$, $RbNiO_2$, and $CsNiO_2$ are currently unavailable. Furthermore, metallic conduction in the Ag_2 plane[18–20] naturally hinders the interaction between the adjacent MO_2 planes through the superexchange interaction via Mn-O-(Ag_2)-O-Mn due to the absence of empty 5s orbital in Ag.[18–20] On the contrary, such interaction via Ni-O-Na-O-Ni is reported to induce interplane AF coupling in $NaNiO_2$.[21] This implies that Ag_2MO_2 is most likely to be a candidate for an ideal 2DTL system.

Indeed, according to our recent muon-spin rotation and relaxation (μ^+SR) experiment,[22] Ag_2NiO_2 was found to exhibit an incommensurate (IC) AF order below 56 K, although $LiNiO_2$ was reported to enter into a spin-glass like state below 10 K (Refs. 15 and 23–26) due to the 3D interaction induced by Ni ions in the Li plane, while $NaNiO_2$ displays an A-type commensurate (C) AF state with $T_N=20$ K that is stabilized by a cooperative Jahn-Teller distortion of the NiO_6 octahedra[27,28] and $AgNiO_2$ displays a C-AF state with $T_N=21$ K caused by slight spatial deviation of the O^{2-} ions.[29] This was also confirmed by very recent μ^+SR ($T_N=19.9$ K) (Ref. 30) and specific-heat measurements ($T_N=19.7$ K).[31] Note that since the Ni^{3+} ions are in a low-spin state with $S=1/2$ ($t_{2g}^6e_g^1$) in the octahedral crystalline electric field of NiO_6, $ANiO_2$ has been thought to be a typical 2DTL with half filling. However, the IC-AF order, which is predicted for the 2DTL with half filling, is only observed for Ag_2NiO_2.[22] The lack of the 3D interaction therefore seems to induce an intrinsic magnetic behavior on the NiO_2 plane.

Among several combinations between Ag_2 and M for AMO_2, only Ag_2NiO_2 and Ag_2MnO_2 have, to authors' knowledge, been prepared thus far. We have therefore naturally extended our μ^+SR experiments to Ag_2MnO_2. Disilver manganese dioxide Ag_2MnO_2 belongs to a monoclinic system with $a=0.5178$ nm, $b=0.2875$ nm, $c=0.8815$ nm, and $\beta=102.3°$ at ambient T (Ref. 20) (see Fig. 1), although it is difficult to obtain more detailed structural data because the c

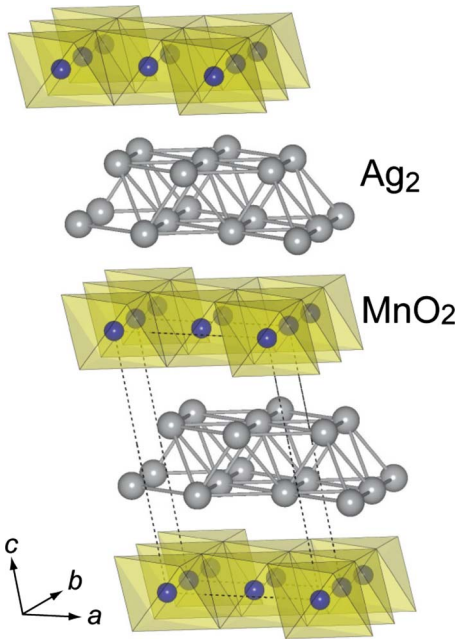

FIG. 1. (Color online) Crystal structure of monoclinic Ag_2MnO_2. The unit cell is plotted by broken lines.

plane of the powder sample is easily aligned by pressing. In spite of its metallic conductivity down to 2 K due to a quarter-filled Ag 5*s* band, as in the case of Ag_2F (Ref. 32) and Ag_2NiO_2,[17,18] the specific-heat (C_p) measurements indicated a transition at $T_{m1}=80$ K, while the susceptibility (χ) measurements showed a spin-glass like transition at $T_{m2}=22$ K under the magnetic field (H) of 1 kOe.[20] Also, both the paramagnetic (PM) Curie temperature (Θ_p) and the effective magnetic moment (μ_{eff}) of Mn ions are estimated as −370 K and $4.93\mu_B$, where the latter value is equivalent to the spin-only value for the Mn^{3+} ions with $S=2$ and $g=2$ [$\mu_{eff}=g\sqrt{S(S+1)}\mu_B$].[20] Very recently, Yoshida *et al.*[20] proposed the possibility of the chirality transition on the 2DTL MnO_2 plane below T_{m1}. However, the microscopic magnetic nature of Ag_2MnO_2, to authors' knowledge, has been less investigated by neutron, NMR, ESR, and μ^+SR measurements thus far.

Among the several magnetic measurement techniques available, μ^+SR is particularly sensitive to the local magnetic environment because the μ^+ mainly feels H_{int} due to its nearest neighbors and is specially sensitive to the short-range magnetic order, which sometimes appears in low-dimensional systems, while both neutron-scattering and χ measurements mainly detect long-range magnetic order; in particular, if the correlation length is very short, neutron-diffraction peaks broaden and eventually disappear.[37]

Here, we report on both weak (relative to the spontaneous internal fields in the ordered state) transverse-field (wTF) and zero-field (ZF) μ^+SRs for a polycrystalline Ag_2MnO_2 sample at temperatures between 1.8 and 300 K. The former method is sensitive to local magnetic order via the shift of the μ^+ spin precession frequency in the applied field and the enhanced μ^+ spin relaxation, while ZF μ^+SR is uniquely sensitive to weak local magnetic disorder in samples exhibiting quasistatic paramagnetic moments.

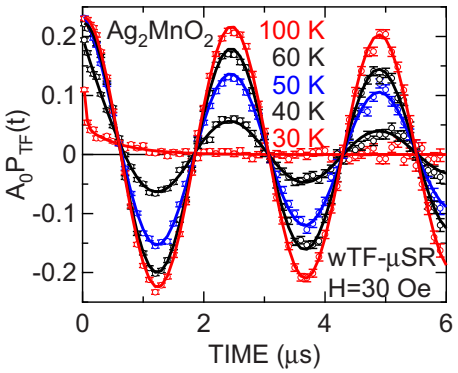

FIG. 2. (Color online) Variation in the wTF-μ^+SR time spectra with T for the Ag_2MnO_2 powder sample. The solid lines show the fitting results using Eq. (1).

II. EXPERIMENT

A powder sample of Ag_2MnO_2 was prepared at the ISSP of the University of Tokyo by a solid-state reaction technique using reagent grade Ag metal and MnO_2 powder as starting materials. A mixture of Ag and MnO_2 was heated at 650 °C for 24 h in an oxygen flow. Then, the calcined powder was ground thoroughly and fired again at 750 °C several times. A more detailed description of the preparation and characterization of the powder is presented in Ref. 20.

Susceptibility (χ) was measured using a superconducting quantum interference device (SQUID) magnetometer (MPMS, Quantum Design) in the temperature range between 400 and 5 K under magnetic field $H\leq 55$ kOe. For the μ^+SR experiments, the powder was pressed into a disk of about 20 mm diameter and 1 mm thickness and subsequently placed in a muon-veto sample holder. The μ^+SR spectra were measured on μE1 (Dolly) surface muon beam line at PSI in Switzerland. The experimental setup and techniques were described elsewhere.[37]

III. RESULTS

A. WTF μ^+SR below 100 K

In order to first roughly assess the nature of the magnetic transition at T_{m1} and T_{m2}, Fig. 2 shows the wTF spectra obtained in a field of 30 Oe at 100, 60, 50, 40, and 30 K on Ag_2MnO_2. As T decreases from 100 K, the oscillation amplitude due to the wTF gradually decreases indicating the appearance of a spontaneous internal field H_{int}. The wTF-μ^+SR spectra were therefore fitted using a combination of a slowly relaxing precessing signal and a fast relaxing nonoscillatory signal. The first component is due to wTF and the latter due to H_{int},

$$A_0P_{TF}(t)=A_{TF}\cos(\omega_{TF}^{\mu}t+\phi_{TF})\exp(-\lambda_{TF}t)+A_{fast}\exp(-\lambda_{fast}t), \quad (1)$$

where A_0 is the initial ($t=0$) asymmetry, $P_{TF}(t)$ is the muon-spin-polarization function, ω_{TF}^{μ} is the muon Larmor frequency corresponding to the applied wTF, ϕ_{TF} is the initial phase of the precessing signal, λ_{TF} and λ_{fast} are the exponen-

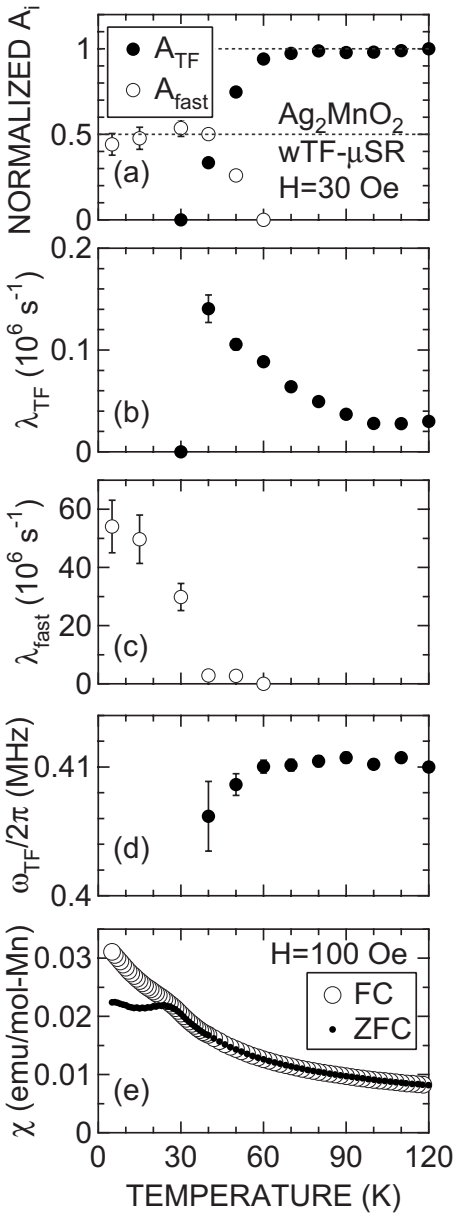

FIG. 3. Temperature dependences of (a) normalized A_{TF} and A_{fast}, (b) TF relaxation rates (λ_{TF}), (c) fast relaxation rate (λ_{fast}), (d) TF frequency ($\omega_{TF}/2\pi$), and (e) susceptibility (χ) for the powder Ag_2MnO_2 sample. The data were obtained by fitting the wTF spectrum using Eq. (1). χ was measured in both zero-field-cooling (ZFC) and field-cooling (FC) modes with $H=100$ Oe.

tial relaxation rates, and A_{TF} and A_{fast} are the asymmetries of the two components of the μ^+SR signal.

Figure 3 shows the T dependences of normalized A_{TF} and A_{fast} ($N_{A_n}=A_n/A_0$; n=TF and fast) [Fig. 3(a)], λ_{TF} [Fig. 3(b)], λ_{fast} [Fig. 3(c)], $\omega_{TF}/2\pi$ [Fig. 3(d)], and χ [Fig. 3(e)]. Upon decreasing T below 100 K, $N_{A_{TF}}$ [which corresponds to the volume fraction (V_F) of PM phases in the sample] shows a clear decrease below 70 K and reaches 0 at 30 K. The T [at which $N_{A_{TF}}$ starts to decrease from its maximum value (=1)] reasonably corresponds to $T_{m1}\sim 80$ K detected by the C_p measurements. Moreover, since $N_{A_{TF}}=0$ below T_{m2} (=30 K), at which the $\chi(T)$ curve obtained in the zero-field-cooling mode exhibits a clear cusp, it is concluded that static order completes below T_{m2}. In contrast, $N_{A_{fast}}$ has a nonzero value below T_{m1} and increases with decreasing T and finally levels off around 0.5 below 30 K. The fact that $N_{A_{fast}}\sim 0.5$ even at 5 K indicates the presence of a large H_{int} below T_{m1} as will be described later. The relaxation of the TF component, $\lambda_{TF}(T)$, shows a monotonic increase below T_{m1} accompanying the decrease observed in $N_{A_{TF}}$, while $\lambda_{fast}(T)$ appears mainly below T_{m2} and increases with decreasing T indicating the evolution of H_{int} below T_{m2}. From the viewpoint of wTF μ^+SR, the two magnetic transitions (T_{m1} and T_{m2}) are therefore assigned to be the onset (T_N^{on}) and end point (T_N^{end}) of the one AF transition with a transition width (ΔT_N) of about 40 K. The midpoint of the transition, at which $N_{A_{TF}}=0.5$, is also estimated as $\sim$45 K.

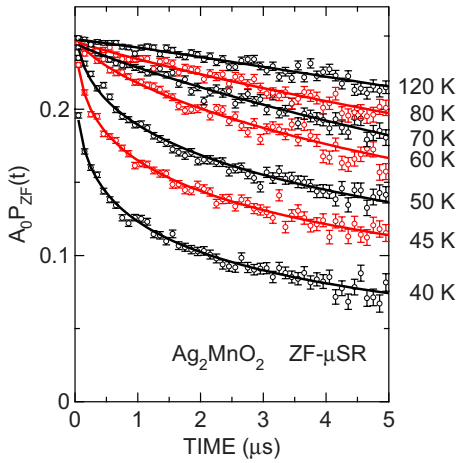

FIG. 4. (Color online) ZF-μ^+SR time spectra in the T range between 40 and 120 K for the Ag_2MnO_2 powder sample. The solid lines show the fitting results using Eq. (2).

Although the C_p measurements showed the peak at the magnetic transition at $T_{m1}(=T_N^{on})$, the entropy change (ΔS_m) from the phase below T_{m1} to the high-T paramagnetic phase was estimated as 0.36 JK^{-1} mol^{-1},[20] which is significantly smaller than the expected value for the $S=2$ system (13.38 JK^{-1} mol^{-1}). This is very consistent with the conclusion from the wTF measurements; that is, disordered moments appear below T_{m1} because the small ΔS_m supports the absence of a conventional second-order AF transition at T_{m1}, below which the whole sample enters into the long-range AF ordered phase.

B. ZF μ^+SR between 40 and 120 K

In order to elucidate the magnetic behavior above T_N^{end}, in particular near $T_N^{on}=\sim 70$ K, we carried out ZF-μ^+SR measurements in the T range between 40 and 120 K (see Fig. 4). In spite of the absence of an oscillatory signal above T_N^{end}, the relaxation rate is found to increase rapidly with decreasing T. Although it is difficult to fit the spectrum using a simple exponential relaxation function [$\exp(-\lambda t)$] in the whole T range between 40 and 120 K, the ZF-μ^+SR spectrum is well fitted by a power exponentially relaxing signal,

$$A_0 P_{ZF}(t) = A_{PE}\exp[-(\lambda_{PE}t)^{\beta}]. \quad (2)$$

Here, "a power exponentially relaxing signal" has been observed for many dense-moment disordered magnetic

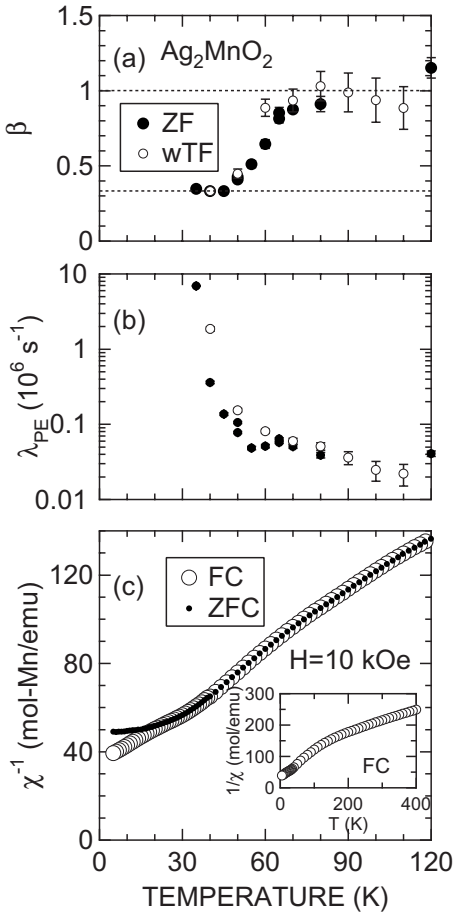

FIG. 5. Temperature dependences of (a) β, (b) λ_{PE}, and (c) χ^{-1} for the Ag_2MnO_2 powder particularly above T_N^{end}. The ZF data were obtained by fitting using Eq. (2), whereas the wTF data using $A_{TF}\cos(\omega_{TF}^{\mu}t+\phi_{TF})\exp[-(\lambda_{PE}t)^{\beta}]$. χ was measured in both ZFC and FC modes with $H=10$ kOe. The inset of (c) shows the $\chi^{-1}(T)$ curve below 400 K.

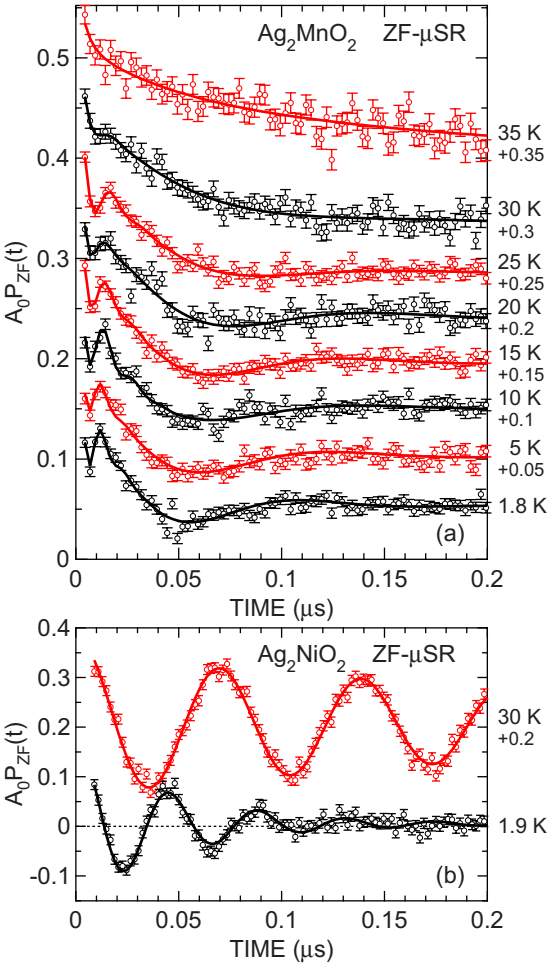

FIG. 6. (Color online) Temperature dependence of the ZF-μ^+SR time spectra of a powder sample of (a) Ag_2MnO_2 and (b) Ag_2NiO_2 (Ref. 22). Each spectrum is offset by (a) 0.05 and (b) 0.2 for clarity of the display. The solid lines in (a) represent the fitting result using Eq. (3). Since the ZF time spectrum for Ag_2MnO_2 is very strongly damped, it is difficult to get a reliable Fourier transform spectrum.

system[33,34] in a paramagnetic state. The fit results are shown in Fig. 5 together with χ^{-1}. As T decreases from 120 K, $\beta \sim 1$ (simple exponential) down to 70 K then β decreases monotonically with further lowering T, dropping below $\beta=0.5$ (root exponential for a dilute-disordered magnet),[35] to finally reach its lowest value (1/3 for a dense-disordered phase).[36] This means a gradual increase in the number density of localized magnetic moments, which are detectable within the muon time scale with decreasing T below T_N^{on}. Accompanying the change in β, λ_{PE} also increases very rapidly below 70 K with decreasing T indicating a broadening of the distribution of H_{int}. This result is therefore consistent with the scenario that disordered moments appear below T_N^{on} and develop with decreasing T, and finally static order completes below T_N^{end}.

Since the slope of the $\chi^{-1}(T)$ curve was found to start to deviate downward from the linear relationship below around 120 K [see the inset of Fig. 5(c)], a FM interaction would contribute in determining the magnetic order in the MnO_2 plane as will be discussed later.

C. ZF μ^+SR below 40 K

Following upon the μ^+SR experiments above 40 K, we measured the ZF-μ^+SR spectrum in order to investigate the detail of H_{int} below T_N. Figure 6 shows ZF-μ^+SR time spectra in an early time domain (below 200 ns) in the T range between 1.8 and 35 K for a powder sample of Ag_2MnO_2. One can clearly see two heavily damped oscillatory components with different frequencies below 30 K; that is, at 1.8 K, one component exhibits the first minimum at around 6 ns and the second minimum at around 18 ns, while the other component shows the first minimum at around 55 ns and the second broad minimum at around 170 ns. This unambiguously establishes the existence of static magnetic order in the sample. However, comparing the result on Ag_2NiO_2 [see Fig. 6(b)],[22] the ZF spectrum for Ag_2MnO_2 is found to be heavily damped even at 1.8 K. This suggests that static order is unlikely long ranged but likely short ranged, although μ^+SR yields no information on correlation length of magnetic order. As T is increased from 1.8 K, the minimum positions shift toward longer times reflecting the expected decrease in

$H_{\rm int}$. Above 35 K, the oscillatory components disappear and the ZF spectrum is just relaxing with time.

We therefore use a combination of two exponentially relaxing cosine oscillation signals and a slow exponential relaxing nonoscillatory signal for fitting the ZF spectrum,

$$A_0 P_{\rm ZF}(t) = A_{\rm AF1}\cos(\omega^{\mu}_{\rm AF1}t+\phi)\exp(-\lambda_{\rm AF1}t) + A_{\rm AF2}\cos(\omega^{\mu}_{\rm AF2}t+\phi)\exp(-\lambda_{\rm AF2}t) + A_{\rm tail}\exp(-\lambda_{\rm tail}t), \quad (3)$$

where $\lambda_{\rm AF1}$, $\lambda_{\rm AF2}$, and $\lambda_{\rm tail}$ are the relaxation rates, $\omega^{\mu}_{\rm AF1}$ and $\omega^{\mu}_{\rm AF2}$ are the muon precession frequencies due to $H_{\rm int}$ [$\omega^{\mu}_{{\rm AF}i}/2\pi = f_{{\rm AF}i} = 13.554$ kHz/Oe($H_{{\rm int}\,i}$)], and ϕ is the initial phase of the precession. The fitting yields $|\phi|$ ranges below 28° well below $T_{\rm N}^{\rm end}$ due to a wide field distribution of $H_{\rm int}$. Although we used a common ϕ for the two cosine oscillations, the fit using two independent ϕ's also provides a similar result, that is, $|\phi_i| \leq 28°$. This suggests commensurate AF order below $T_{\rm N}^{\rm end}$ because the cosine fit for an IC field should yield $\phi = -45°$ for the both cosine functions,[37,38] as muons locate at the sites that are commensurate to the lattice. The $A_{\rm tail}$ signal corresponds to the "1/3 tail" caused by the AF field component parallel to the initial muon-spin polarization [$\boldsymbol{S}_{\mu}(0)$].

Figures 7(a)–7(d) show the T dependence of the muon precession frequencies ($f_{{\rm AF}i} = \omega^{\mu}_{{\rm AF}i}/2\pi$), the normalized $A_{{\rm AF}i}$, $A_{\rm tail}$, and $A_{\rm TF}$, the exponential relaxation rates $\lambda_{\rm AF1}$ and $\lambda_{\rm AF2}$, and the ratio of the precession frequencies and amplitudes of the two oscillatory signals, i.e., $T_{\rm N}$ and $A_{\rm AF1}/A_{\rm AF2}$ for the powder sample of Ag_2MnO_2. As T decreases from $T_{\rm N}^{\rm end}$, both $f_{\rm AF1}$ and $f_{\rm AF2}$ increase with decreasing slope ($|df_{{\rm AF}i}/dT|$) and roughly level off at their highest values below about 20 K. Here, the $f_{\rm AF1}(T)$ curve seems to be very similar to the $f_{\rm AF2}(T)$ curve, although $f_{\rm AF1}$ is larger by one order of magnitude than $f_{\rm AF2}$ in the whole T range below $T_{\rm N}^{\rm end}$. This means that the two $f_{{\rm AF}i}$'s are not caused by two different AF phases but by two different muon sites in the AF ordered lattice.

The $A_{\rm AF1}(T)$ and $A_{\rm AF2}(T)$ curves are almost independent of T except at the vicinity below $T_{\rm N}^{\rm end}$. The population of the two muon sites is therefore not altered with T. This is in good agreement with the fact that muons form a stable bond with O^{2-} ions at low T. Furthermore, $A_{\rm tail}$ is roughly a constant (~0.2) at T below $T_{\rm N}^{\rm end}$, which is consistent with the behavior of the 1/3 tail, although the magnitude of $A_{\rm tail}$ is smaller than the predicted value for a powder sample (1/3). This is probably due to the preferred orientation of the pressed powder sample.[20] On the contrary, since the c plane tends to align by pressing because of the 2D structural nature of Ag_2MnO_2, the smaller $A_{\rm tail}$ for the pressed powder than that for a random powder (1/3) would imply that $H_{\rm int} \perp c$ as $\boldsymbol{S}_{\mu}(0)$ is perpendicular to the basal plane. Note that all the three ZF signals appear below $T_{\rm N}^{\rm end}$, at which $A_{\rm TF}$ reaches 0. This strongly supports that $T_{\rm m2} = T_{\rm N}^{\rm end}$.

The two relaxation rates ($\lambda_{\rm AF1}$ and $\lambda_{\rm AF2}$) are also roughly T independent below $T_{\rm N}^{\rm on}$, suggesting that the field distribution is fixed at $T_{\rm N}^{\rm on}$ and is not developed with decreasing T. Indeed, the shape of the ZF-μ^+SR spectrum at 25 K is essentially the same as that at 1.8 K, whereas the minimum positions delay with increasing T. In general, as T decreases,

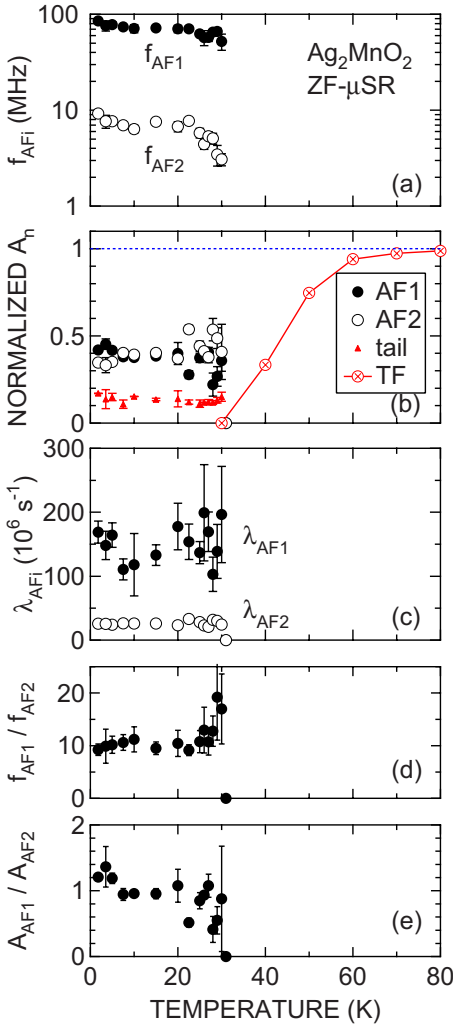

FIG. 7. (Color online) Temperature dependences of (a) the muon precession frequencies ($f_{{\rm AF}i} = \omega^{\mu}_{{\rm AF}i}/2\pi$), (b) the normalized $A_{{\rm AF}i}$, $A_{\rm tail}$, and $A_{\rm TF}$, (c) the exponential relaxation rates $\lambda_{\rm AF1}$ and $\lambda_{\rm AF2}$, (d) $f_{\rm AF1}/f_{\rm AF2}$, and (e) $A_{\rm AF1}/A_{\rm AF2}$ for the powder sample of Ag_2MnO_2. The data were obtained by fitting the ZF spectrum using Eq. (3), while the normalized $A_{\rm TF}$ is the same to that seen in Fig. 3(a).

a relaxation rate of an AF oscillation signal naturally decreases due to the decrease in thermal fluctuations. The T-independent $\lambda_{{\rm AF}i}$ hence would suggest the existence of the other parameter for determining the field distribution of AF order for Ag_2MnO_2. Geometrical frustration on 2DTL could be such parameter for details are still unknown.

If we ignore the change in $f_{\rm AF1}/f_{\rm AF2}$ at the vicinity below $T_{\rm N}^{\rm end}$, $f_{\rm AF1}/f_{\rm AF2}$ is found to be ~10 in the whole T range in the AF phase. The ratio between $A_{\rm AF1}$ and $A_{\rm AF2}$ is also approximately equal to 1 in the AF phase. The most reasonable scenario to explain these results is that, although there is only one muon site in the crystallographic lattice, there are two magnetically different muon sites in the AF ordered state. The population of one site is almost equivalent to that of the other site, whereas the $H_{\rm int}$ at one site is ten times larger than that at the other site. This issue will be discussed later.

We therefore attempted to fit all the ZF spectra below $T_{\rm N}^{\rm end}$ using common ϕ, $A_{\rm AF1}$, $A_{\rm AF2}$, $A_{\rm tail}$, and $f_{\rm AF1}/f_{\rm AF2}$ in Eq. (3)

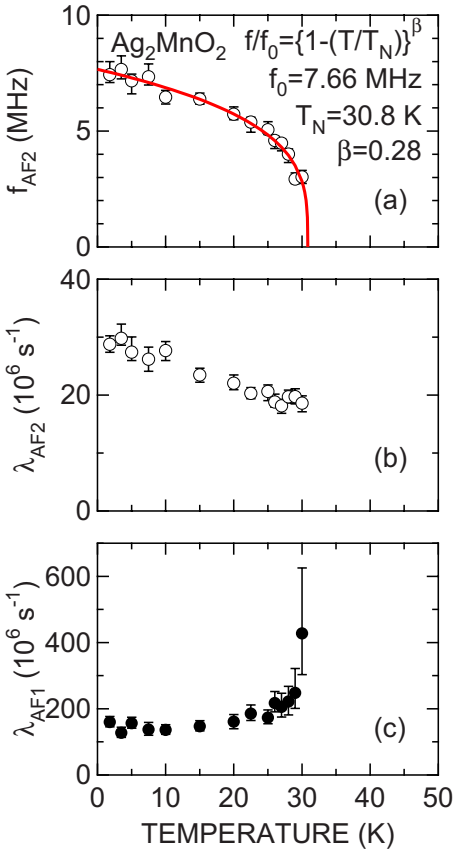

FIG. 8. (Color online) Temperature dependences of (a) f_{AF2}, (b) λ_{AF2}, and (c) λ_{AF1} for the powder sample of Ag_2MnO_2. The data were obtained by fitting the 14 ZF spectra below T_N^{end} using common ϕ, A_{AF1}, A_{AF2}, A_{tail}, and f_{AF1}/f_{AF2} for Eq. (3). The solid line in (a) represents the fitting result using Eq. (4).

because $|\phi_i| \leq 28°$ and the rest parameters are almost T independent as seen in Fig. 7. The "global fit" provided that $\phi = -8 \pm 5°$, $A_{AF1} = 0.1027 \pm 0.0008$, $A_{AF2} = 0.0935 \pm 0.0012$ ($A_{AF1}/A_{AF2} = 1.07 \pm 0.05$), $A_{tail} = 0.0263 \pm 0.0008$, and $f_{AF1}/f_{AF2} = 11.7 \pm 0.4$, respectively. Figure 8 shows the T dependences of f_{AF2}, λ_{AF2}, and λ_{AF1} obtained by the global fit. The $f_{AF2}(T)$ curve, which is the T dependence of an order parameter of the transition, is well fitted by the following expression:

$$f_{AF}(T) = f_{AF}(0\ \mathrm{K})\left(\frac{T_N - T}{T_N}\right)^{\beta_m}. \quad (4)$$

This provides $f_{AF2}(0\ \mathrm{K}) = 7.66 \pm 0.14$ MHz, $T_N(=T_N^{end}) = 30.8 \pm 0.5$ K, and $\beta_m = 0.28 \pm 0.03$ [see Fig. 8(a)]. The exponent (β_m) obtained is comparable to the predictions for the 2D xy model on a triangular lattice ($\beta_m = 0.25 \pm 0.02$),[39,40] although we need more accurate data in the vicinity of T_N to determine β_m more precisely. Also, the obtained value for Ag_2MnO_2 is 15% larger than β_m for $NaNiO_2$ estimated by μ^+SR measurements (0.24 ± 0.01) (Ref. 27) and is almost comparable to β_m for $Na_{0.75}CoO_2$ (~ 0.28).[41]

IV. DISCUSSION

Although the AF spin structure has not been solved yet, here we show that we can exclude several possible AF structures from the present μ^+SR results. Note that since the structural data at low T is unavailable, we assume that there are no structural phase transitions down to the lowest T measured. This is consistent with the results of the C_p and χ measurements.[20]

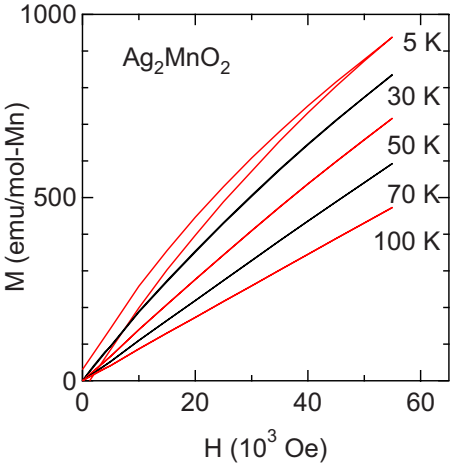

FIG. 9. (Color online) Magnetization (M) vs magnetic field (H) for Ag_2MnO_2 at several temperatures. Although M was measured both on increasing H and on decreasing H, the MH hysteresis is only observed below 30 K.

The relationship between magnetization (M) and H exhibits hysteresis only below T_N (Fig. 9). This could imply that the Mn spins freeze below T_N. However, the two oscillations in the ZF spectrum (see Fig. 6), even if there are only first two minima for the both oscillations, clearly demonstrate the formation of static AF order below T_N. Furthermore, although the ac-$\chi(T)$ curve shows a cusp at T_N as in the case of dc χ, the T of the cusp is found to be independent of the ac frequency.[42] This strongly supports the static AF order for Ag_2MnO_2 at low T.

Moreover, the cosine fit rules out the possibility of IC-spin-density wave (SDW) order below T_N, which is in contrast to the case of Ag_2NiO_2. Actually, the T-independent f_{AF1}/f_{AF2} and A_{AF1}/A_{AF2} below T_N are reasonably explained by the coexistence of two magnetically different muon sites in the C-AF ordered lattice. On the other hand, if we assume the IC-SDW field, f_{AF1} and f_{AF2} naturally correspond to the upper and lower limits of the field distribution. The relative field distribution width $[1-(f_{AF2}/f_{AF1})]$ should thus be T independent. However, the wave vector of IC-SDW often depends on T.[43] This naturally implies the change in the IC field distribution with T resulting in the "T dependence" of f_{AF1}/f_{AF2} and A_{AF1}/A_{AF2}. Therefore, we decided that the phase below T_N is a static but short-range C-AF ordered phase.

Next we discuss the case for chirality order on the 2DTL MnO_2 plane (see Fig. 10) proposed by the recent C_p and χ measurements.[20] As is well known, μ^+SR is very sensitive to the local magnetic environment. Hence, if the chirality ordered state appears in the MnO_2 plane, we could expect to observe the damped oscillations in the ZF spectrum as we have already obtained in Fig. 6, although the chirality ordered state was originally proposed for the phase in the T range between T_N^{on} and T_N^{end}.[20] At first, it should be noted that

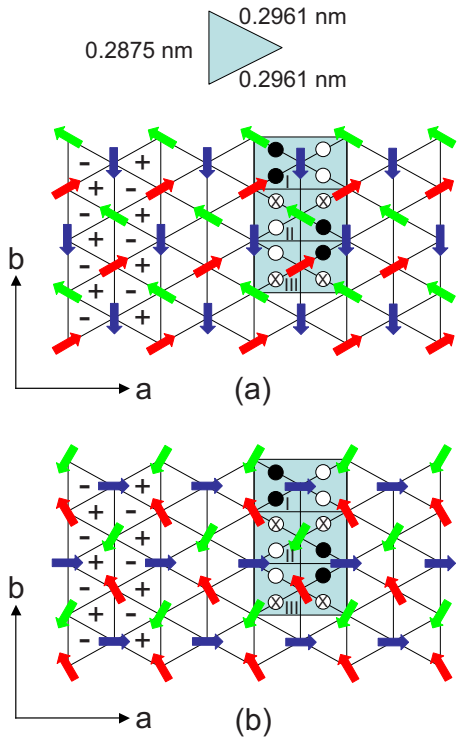

FIG. 10. (Color online) The distortion of the Mn triangular lattice (top) and the ground state of the antiferromagnetic triangular lattice (a) with xy spins and (b) with a 120° spin structure. The positive and negative chiralities are indicated by + and −. Solid (I), open (II), and crossed (III) circles represent the muon's sites located at a distance of 1.7 Å above or below the Mn plane. The rectangular region in (a) and (b) shows the structural and magnetic unit cells, where the latter is three times larger than the former along the b axis.

the triangular lattice of Ag_2MnO_2 is slightly distorted from the regular triangle to the isosceles triangle as seen in the top of Fig. 10. The length of the bottom edge, which is parallel to the b axis, is shorter by ~3% than that of the rest two edges. According to electrostatic-potential calculations using the atomic positions for Ag_2NiO_2 but lattice parameters for Ag_2MnO_2, μ^+'s are most likely to locate at the middle of the two long edges of the Mn triangular lattice but above or below the Mn plane about 1.7 Å away.

Then, simple dipole field calculations yield that there are three magnetically different μ^+'s sites represented by solid (I), open (II), and crossed (III) circles in Fig. 10. When a magnitude of the Mn moment (μ_{Mn}) is $1\mu_B$, $H_{int,I}=1965$ Oe, $H_{int,II}=1927$ Oe, and $H_{int,III}=792$ Oe with the muon occupancy ratio $H_{int,I}:H_{int,II}:H_{int,III}=1:1:1$. If we assume that μ_{Mn} is comparable to $\mu_{eff}(=4.93\mu_B)$, three oscillation frequencies would be observed in the ZF spectrum at $f_I=131$ MHz, $f_{II}=129$ MHz, and $f_{III}=53$ MHz for the chirality ordered phase [Fig. 10(a)]. In contrast, the present μ^+SR gives two quite different frequencies (one is 11.7 times larger than the other) with almost equal number of densities [see Figs. 7(d) and 7(e)].

It is, thus, very difficult to explain the present μ^+SR data based only on the μ^+'s sites at the vicinity of the MnO_2 plane. Therefore, we considered two crystallographically different μ^+ sites in the Ag_2MnO_2 lattice in order to explain the two f signals. That is, one is the site shown in Fig. 10 (IV =I, II and III) and the other is the interstitial site in the metallic Ag_2 plane (V) as in the case of metals and/or alloys.[37] The calculations provide that $H_{int,IV}/\mu_{Mn}=1600\pm700$ Oe/$\mu_B=1/3\Sigma_{i=I}^{III}(H_{int,i}/\mu_{Mn})$, $H_{int,V}/\mu_{Mn}=60\pm20$ Oe/μ_B, and $H_{int,IV}/H_{int,V}=30\pm40$, respectively. The wide field distribution of the two H_{int}'s is consistent with the heavily damped oscillation in the ZF spectrum. However, even if $\mu_{Mn}=\mu_{eff}$, the magnitude of $H_{int,V}=300\pm100$ Oe, which corresponds to $f_{int,V}=4.1\pm1.4$ MHz, is about half of the experimental result [$f_{AF2}(0\ K)\sim7.7$ MHz]. Here, considering a large estimation error for $H_{int,IV}/H_{int,V}$ due to the wide field distribution of each H_{int}, the calculated ratio is not crucial to judge the formation of the chirality ordered phase below T_N. Furthermore, the μ^+ occupancy at site IV should be accidentally equivalent to that at site V, while the vicinity of O^{2-} ions (site IV) is thought to be most stable for μ^+. Finally, it should be noted that the ZF-μ^+SR spectra for Ag_2NiO_2, which has almost the same crystal structure and charge distribution as Ag_2MnO_2, exhibits a very clear oscillation with two similar frequency components, i.e., 22 and 26 MHz at 1.9 K.[22] If we assume that μ^+'s sit at site V in Ag_2MnO_2, μ^+'s are naturally likely to do so also in Ag_2NiO_2. However, the estimated ratio of the two frequencies is too small to explain the result of Ag_2NiO_2, and therefore μ^+'s are most unlikely to sit at site V both in Ag_2NiO_2 and Ag_2MnO_2. These suggest that the chirality order is unlikely to explain the present result.

The calculations were also performed for the following spin arrangements and the results are listed in Table I: (i) Chirality ordered phase with 120° spin structure [see Fig. 10(b)]. (ii) Collinear phase, in which the spins are aligned parallel to the b axis, i.e., the FM chain is formed along the b axis, but the neighboring FM chains are antiparallel to each other. (iii) A-type AF phase. Nevertheless, there is no reasonable spin arrangement for explaining the magnitude of f_{AF1} and the ratio of $f_{AF1}/f_{AF2}(\sim11.7)$ and $A_{AF1}/A_{AF2}(\sim1.07)$, simultaneously.

For the A-type AF case, the H_{int} (f_μ) ratio between sites IV and V is calculated as 16.3, which is the most proximate to the experimental result (11.7). We thus discuss the possibility of A-type AF order in detail. At first, we should note that even if $\mu_{Mn}=\mu_{eff}$, the magnitude of $f_{int,IV}(\sim43$ MHz) for A-type AF order is about half of the experimental result [$f_{AF1}(0\ K)\sim90$ MHz]. The question on the occupancy ratio between sites IV and V still remains the same to the case of the chirality ordered phase as mentioned above. If we ignore these inconsistency, although $\Theta_p=-370$ K, the FM contribution observed in the $\chi^{-1}(T)$ curve below ~120 K would support an FM arrangement of the Mn spins in the MnO_2 plane as predicted theoretically for $LiNiO_2$.[44] For the A-type AF order state, past μ^+SR work, however, reported a very clear oscillation with small damping as in the case of $NaNiO_2$ (Ref. 27) and $Na_{0.75}CoO_2$.[2,41,45,46] Actually, the present calculation also predicts only one f signal for μ^+'s at site IV. Hence, a very clear oscillation is expected to be observed in the ZF spectrum, which is in contrast to the experimental result. These suggest that the A-type AF order is most unlikely to explain the present result.

TABLE I. Dipole field $H_{\mathrm{int}}/\mu_{\mathrm{Mn}}$ (top), muon precession frequency f_μ/μ_{Mn} (middle), and muon occupancy ratio R_{mo} (bottom) at the muon sites I–V in several ordered structures. Here, site I is crystallographically the same as sites II and III (see Fig. 10). When site I is thought to be magnetically the same as sites II and III, sites I, II, and III are represented by site IV. For such case, the interstitial site in the metallic Ag_2 plane (site V) is considered in order to explain the two f signals. Since H_{int} (f_μ) is proportional to the ordered moment (μ_{Mn}), its unit is given by Oe/μ_B (MHz/μ_B). Assuming that $\mu_{\mathrm{Mn}}=\mu_{\mathrm{eff}}=4.93\mu_B$, the highest H_{int} (f_μ) is equivalent to $4.93(H_{\mathrm{int}}/\mu_{\mathrm{Mn}})$ $[4.93(f_\mu/\mu_{\mathrm{Mn}})]$. Here, $f_\mu=H_{\mathrm{int}}(13.554$ kHz/Oe). We also calculated H_{int} for site IV′, which is the middle of one short edge of the Mn triangular lattice (see the top of Fig. 10) and is more unstable than site IV according to electrostatic-potential calculations. For the collinear spin structure, $H_{\mathrm{int,IV}}/H_{\mathrm{int,IV'}}=7.96$ and $R_{\mathrm{mo,IV}}/R_{\mathrm{mo,IV'}}=2$ (11.7 and 1.07 from the experiment), if we assume that the electrostatic potential for site IV′ is equivalent to that for site IV. For the other spin structures, muons at site IV′ give an additional field distribution width to $H_{\mathrm{int,IV}}$ but do not produce the two quite different H_{int}'s. Therefore, even if we consider the contribution of the muons at site IV′, it is still difficult to explain the experimental result.

Structure		Site I	Site II	Site III	Site IV	Site IV′	Site V
Chiral xy	$H_{\mathrm{int}}/\mu_{\mathrm{Mn}}$ (Oe/μ_B)	1965	1927	792	1600 ± 700	1400 ± 700	60 ± 20
[See Fig. 10(a)]	f_μ/μ_{Mn} (MHz/μ_B)	26.6	26.1	10.73	21 ± 9	20 ± 9	0.8 ± 0.3
	R_{mo}	1/3	1/3	1/3	1	1/2	?
Chiral 120°	$H_{\mathrm{int}}/\mu_{\mathrm{Mn}}$ (Oe/μ_B)	1324	1268	2200	1600 ± 500	1500 ± 500	61 ± 19
[See Fig. 10(b)]	f_μ/μ_{Mn} (MHz/μ_B)	17.95	17.19	29.8	22 ± 7	20 ± 7	0.8 ± 0.3
	R_{mo}	1/3	1/3	1/3	1	1/2	?
Collinear	$H_{\mathrm{int}}/\mu_{\mathrm{Mn}}$ (Oe/μ_B)				1098	138	923
FM along b but AF along a	f_μ/μ_{Mn} (MHz/μ_{B})				14.88	1.87	12.51
	R_{mo}				1	1/2	?
A-type AF	$H_{\mathrm{int}}/\mu_{\mathrm{Mn}}$ (Oe/μ_B)				652	490	40
FM in the plane but AF along c	f_μ/μ_{Mn} (MHz/μ_B)				8.84	6.64	0.54
	R_{mo}				1	1/2	?

Interestingly, a fast relaxing signal is also reported to appear in the ZF spectrum below ~24 K for $NaNiO_2$,[27] whereas $T_{\mathrm{N}}=20$ K. On the other hand, such signal does not exist above T_{N} for $Na_{0.75}CoO_2$. Indeed, as T decreases from 30 K, the $A_{\mathrm{TF}}(T)$ curve for $Na_{0.75}CoO_2$ exhibits a very sharp drop (a steplike decrease) at $T_{\mathrm{N}}=22$ K.[41] Therefore, the appearance of the fast relaxing signal above T_{N}, which is observed in Ag_2MnO_2, is unlikely to correlate the formation of A-type AF order.

In conclusion, although we can exclude the A-type AF and collinear ordered phases from the present μ^+SR result, the magnetic structure is still not completely elucidated. In order to further understand the AF spin structure below $T_{\mathrm{N}}^{\mathrm{end}}$, μ^+SR experiments using single crystals or aligned powder samples are required to know the magnetic anisotropy of Ag_2MnO_2. Furthermore, neutron-scattering measurements would provide additional crucial information on existence/absence of AF order below $T_{\mathrm{N}}^{\mathrm{end}}$, given its different spatial and time resolution from those of μ^+SR. Moreover, a detailed structural analysis, preferably in a synchrotron-radiation source, would yield significant information on the possible slight displacement of O ions and/or the small distortion of the triangular lattice, which could be undetectable by the C_p and χ measurements.

V. SUMMARY

A positive muon-spin rotation/relaxation (μ^+SR) experiment on a powder sample of Ag_2MnO_2, in which Mn ions form the two-dimensional triangular lattice in the MnO_2 plane, has demonstrated the existence of a static but short-ranged AF order below $T_{\mathrm{N}}^{\mathrm{end}}=30$ K, while disordered moments appear below $T_{\mathrm{N}}^{\mathrm{on}}=80$ K. The strongly damped oscillatory signal in the ZF spectrum, however, indicates a wide field distribution at the muon sites even at 1.8 K due to the geometrical frustration of the triangular lattice. Although the AF spin structure is still unknown, since the Ag_2 plane is expected to reduce or eventually annihilate the interplane

interaction between the adjacent MnO_2 planes, further studies of the magnetic properties of the MnO_2 plane particularly the ground state of the AF phase should yield significant information on the physics of these unique frustrated systems.

ACKNOWLEDGMENTS

This work was performed at the Swiss Muon Source, Paul Scherrer Institut, Villigen, Switzerland. We thank the staff of PSI for their help with the μ^+SR experiments. We also appreciate Jess H. Brewer of University of British Columbia and Eduardo J. Ansaldo of TRIUMF for their fruitful discussions. Y.I., H.N., and J.S. are partially supported by the KEK-MSL Inter-University Program for Oversea Muon Facilities. This work is also supported by Grant-in-Aid for Scientific Research (B), MEXT, Japan under Grant No. 19340107.

*e0589@mosk.tytlabs.co.jp

[1] T. A. Hewston and B. L. Chamberland, J. Phys. Chem. Solids **48**, 97 (1987), and references cited therein.
[2] J. Sugiyama, J. H. Brewer, E. J. Ansaldo, H. Itahara, T. Tani, M. Mikami, Y. Mori, T. Sasaki, S. Hébert, and A. Maignan, Phys. Rev. Lett. **92**, 017602 (2004).
[3] J. Sugiyama, H. Nozaki, Y. Ikedo, K. Mukai, J. H. Brewer, E. J. Ansaldo, G. D. Morris, D. Andreica, A. Amato, T. Fujii, and A. Asamitsu, Phys. Rev. Lett. **96**, 037206 (2006).
[4] K. Mukai, Y. Ikedo, H. Nozaki, J. Sugiyama, K. Nishiyama, D. Andreica, A. Amato, P. L. Russo, E. J. Ansaldo, J. H. Brewer, K. H. Chow, K. Ariyoshi, and T. Ohzuku, Phys. Rev. Lett. **99**, 087601 (2007).
[5] K. Takada, H. Sakurai, E. Takayama-Muromachi, F. Izumi, R. A. Dilanian, and T. Sasaki, Nature (London) **422**, 53 (2003).
[6] C. Darie, P. Bordet, S. de Brion, M. Holzapfel, O. Isnard, A. Lecchi, J. E. Lorenzo, and E. Suard, Eur. Phys. J. B **43**, 159 (2005).
[7] M. J. Lewis, B. D. Gaulin, L. Filion, C. Kallin, A. J. Berlinsky, H. A. Dabkowska, Y. Qiu, and J. R. D. Copley, Phys. Rev. B **72**, 014408 (2005).
[8] S. P. Bayrakci, I. Mirebeau, P. Bourges, Y. Sidis, M. Enderle, J. Mesot, D. P. Chen, C. T. Lin, and B. Keimer, Phys. Rev. Lett. **94**, 157205 (2005).
[9] L. M. Helme, A. T. Boothroyd, R. Coldea, D. Prabhakaran, D. A. Tennant, A. Hiess, and J. Kulda, Phys. Rev. Lett. **94**, 157206 (2005).
[10] H. R. Krishnamurthy, C. Jayaprakash, S. Sarker, and W. Wenzel, Phys. Rev. Lett. **64**, 950 (1990).
[11] M. Fujita, M. Ichimura, and K. Nakao, J. Phys. Soc. Jpn. **60**, 2831 (1991).
[12] M. Fujita, T. Nakanishi, and K. Machida, Phys. Rev. B **45**, 2190 (1992).
[13] M. C. Refolio, J. M. López Sancho, and J. Rubio, Phys. Rev. B **65**, 075114 (2002).
[14] T. Koretsune and M. Ogata, Phys. Rev. Lett. **89**, 116401 (2002).
[15] J.-H. Chung, Th. Proffen, S. Shamoto, A. M. Ghorayeb, L. Croguennec, W. Tian, B. C. Sales, R. Jin, D. Mandrus, and T. Egami, Phys. Rev. B **71**, 064410 (2005).
[16] Y. J. Shin, J. P. Doumerc, P. Dordoe, C. Delmas, M. Pouchard, and P. Hagenmuller, J. Solid State Chem. **107**, 303 (1993).
[17] M. Schreyer and M. Jansen, Angew. Chem. **41**, 643 (2002).
[18] H. Yoshida, Y. Muraoka, T. Sörgel, M. Jansen, and Z. Hiroi, Phys. Rev. B **73**, 020408(R) (2006).
[19] G. Rienäcker and K. Werner, Z. Anorg. Allg. Chem. **320**, 141 (1963).
[20] H. Yoshida, S. Ahlert, M. Jansen, Y. Okamoto, J. Yamaura, and Z. Hiroi, J. Phys. Soc. Jpn. **77**, 074719 (2008).
[21] A. J. W. Reitsma, L. F. Feiner, and A. M. Olés, New J. Phys. **7**, 121 (2005).
[22] J. Sugiyama, Y. Ikedo, K. Mukai, J. H. Brewer, E. J. Ansaldo, G. D. Morris, K. H. Chow, H. Yoshida, and Z. Hiroi, Phys. Rev. B **73**, 224437 (2006).
[23] Y. Kitaoka, T. Kobayashi, A. Koda, H. Wakabayashi, Y. Niino, H. Yamakage, S. Taguchi, K. Amaya, K. Yamaura, M. Takano, A. Hirano, and R. Kanno, J. Phys. Soc. Jpn. **67**, 3703 (1998).
[24] T. Chatterji, W. Henggeler, and C. Delmas, J. Phys.: Condens. Matter **17**, 1341 (2005).
[25] J. N. Reimers, J. R. Dahn, J. E. Greedan, C. V. Stager, G. Liu, I. Davidson, and U. Von Sacken, J. Solid State Chem. **102**, 542 (1993).
[26] According to the recent μ^+SR experiment, Li_xNiO_2 with $0.6 \leq x \leq 1$ was found to enter into a short-ranged A-type AF ordered phase at low T; J. Sugiyama, K. Mukai, Y. Ikedo, P. L. Russo, H. Nozaki, D. Andreica, A. Amato, K. Ariyoshi, and T. Ohzuku, Phys. Rev. B (to be published).
[27] P. J. Baker, T. Lancaster, S. J. Blundell, M. L. Brooks, W. Hayes, D. Prabhakaran, and F. L. Pratt, Phys. Rev. B **72**, 104414 (2005).
[28] H. Meskine and S. Satpathy, Phys. Rev. B **72**, 224423 (2005).
[29] E. Wawrzyńska, R. Coldea, E. M. Wheeler, I. I. Mazin, M. D. Johannes, T. Sörgel, M. Jansen, R. M. Ibberson, and P. G. Radaelli, Phys. Rev. Lett. **99**, 157204 (2007).
[30] T. Lancaster, S. J. Blundell, P. J. Baker, M. L. Brooks, W. Hayes, F. L. Pratt, R. Coldea, T. Sörgel, and M. Jansen, Phys. Rev. Lett. **100**, 017206 (2008).
[31] E. Wawrzyńska, R. Coldea, E. M. Wheeler, T. Sörgel, M. Jansen, R. M. Ibberson, P. G. Radaelli, and M. Koza, Phys. Rev. B **77**, 094439 (2008).
[32] K. Andres, N. A. Kuebler, and M. B. Robin, J. Phys. Chem. Solids **27**, 1747 (1966).
[33] D. R. Noakes, G. M. Kalvius, R. Wappling, C. E. Stronach, M. F. White, Jr., H. Saito, and K. Fukamichi, Phys. Lett. A **238**, 197 (1998).
[34] D. R. Noakes, G. M. Kalvius, and O. Hartmann, Phys. Rev. B **65**, 132413 (2002).
[35] Y. J. Uemura, T. Yamazaki, R. S. Hayano, R. Nakai, and C. Y. Huang, Phys. Rev. Lett. **45**, 583 (1980).
[36] A. T. Ogielski, Phys. Rev. B **32**, 7384 (1985).
[37] G. M. Kalvius, D. R. Noakes, and O. Hartmann, in *Handbook on the Physics and Chemistry of Rare Earths*, edited by K. A. Gschneidner, Jr., L. Eyring, and G. H. Lander (North-Holland,

Amsterdam, 2001), Vol. 32, Chap. 206.
[38] D. Andreica, Ph.D. thesis, IPP/ETH-Zurich, 2001.
[39] H. Kawamura, J. Appl. Phys. **63**, 3086 (1988), and references cited therein.
[40] A. Taroni, S. T. Bramwell, and P. C. W. Holdsworth, J. Phys.: Condens. Matter **20**, 275233 (2008).
[41] P. Mendels, D. Bono, J. Bobroff, G. Collin, D. Colson, N. Blanchard, H. Alloul, I. Mukhamedshin, F. Bert, A. Amato, and A. D. Hillier, Phys. Rev. Lett. **94**, 136403 (2005).
[42] Z. Hiroi (private communication).
[43] G. Grüner, *Density Waves in Solids* (Addison-Wesley-Longmans, Reading, MA, 1994), Chap. 4.
[44] T. Arimori and S. Miyashita, J. Phys. Soc. Jpn. **69**, 2250 (2000).
[45] J. Sugiyama, H. Itahara, J. H. Brewer, E. J. Ansaldo, T. Motohashi, M. Karppinen, and H. Yamauchi, Phys. Rev. B **67**, 214420 (2003).
[46] S. P. Bayrakci, C. Bernhard, D. P. Chen, B. Keimer, R. K. Kremer, P. Lemmens, C. T. Lin, C. Niedermayer, and J. Strempfer, Phys. Rev. B **69**, 100410(R) (2004).